Characterization of highly selective & CNS-penetrant PARP1 inhibitors

Cowley PM, McGuinness BE, Campbell GM and Wise A#

Duke Street Bio Ltd, 2 Duke St, London, UK

Abstract 35678 2023

Background

First-generation PARP1 inhibitors have provided significant therapeutic benefit to patients whose tumours exhibit homologous repair deficiencies, including those harbouring BRCA mutations. However, their use has been associated with haematological toxicities that have restricted their application, particularly in combination with standard-of-care chemotherapy. All four FDA-approved PARP1 inhibitors are largely non-selective for the closely related enzyme PARP2, inhibition of which has been shown to drive haematotoxicity. Hence, the development of second-generation molecules highly selective for PARP1 over PARP2 offers a significant opportunity to

1) dramatically enhance therapeutic index,
2) enable additional precision medicine / combination approaches with chemotherapy, radiotherapy, immunotherapy and targeted agents and
3) expand the addressable patient population to those whose tumours carry additional DDR defects.

We have discovered two novel series of exquisitely PARP1-selective, CNS-penetrant inhibitors using X-ray crystallography and structure-based design. Herein we describe their characterization, exemplified by DSB2455 and DSB3218.

In vitro Potency & ADME

		DSB2455	DSB3218	Olaparib	AZD5305	AZD9574
PARP1 Biochemical Binding (PARP2 Selectivity)	K_D (nM)	0.6 (1,300-fold)	0.7 (339-fold)	0.8 (0.6-fold)	0.7 (60-fold)	0.95 (>5,000-fold)
PARP1 NanoBRET[1] (PARP2 Selectivity)		1.1 (>4,000-fold)	0.9 (1,445-fold)	3.0 (0.7-fold)	1.6 (180-fold)	2.3 (>5,000-fold)
MDA-MB-436 (BRCA1m)						
7 Day Viability (Cell Titer Glo)	IC_{50} (nM)	3	4	26	1	12
14 Day Colony Forming Unit Inhibition		0.05	0.06	0.5	0.1	0.09
P-γH2AX Induction		6	3	26	2	1
PARylation Inhibition		4	8	34	7	7
DLD1 BRCA2$^{-/-}$						
7 Day Viability (Cell Titer Glo)	IC_{50} (nM)	7	2	65	2	4
14 Day Colony Forming Unit Inhibition		0.2	0.2	2.5	0.3	0.2
P-γH2AX Induction		3	4	-	2	2
PARP1 Chromatin Trapping		1.9	3.6	39	0.7	4.2
Mics CLint (µL/min/mg) / Heps CLint (µL/min/10^6 cells)		<7.4	<1.9	<7.4	5.4	
Plasma Stability $T_{1/2}$ (mins) / Plasma Protein Binding (%)		>373	88.6	>373	81.5	
CYP Inhibition, 5 isoforms (µM)		>50		>50		
CYP Time-Dependent Inhibition (µM)		>50		>50		
Caco-2 (10^{-6} cm/s) A→B / Efflux Ratio		4.7	5.4	14.0	2.1	
MDCK-MDR1 (10^{-6} cm/s) A→B / Efflux Ratio		1	15.6	2.8	8.5	

Table 1. DSB2455 & DSB3218 are potent inhibitors of PARP1 in biochemical and cell-based assays with high selectivity over PARP2, while demonstrating excellent *in vitro* ADME properties.

[1]Assay performed at Proteros Biostructures GmbH

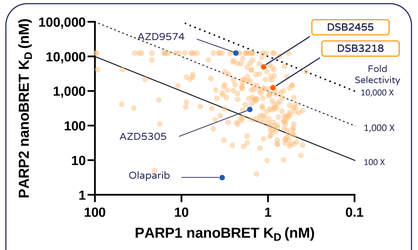

Fig. 1. DSB2455 & DSB3218 demonstrate high PARP1 selectivity over PARP2 in a cell-based NanoBRET[1] target engagement assay.

Table 2. DSB2455 demonstrates excellent *in vivo* PK

	Mouse	Rat	Dog
V_{SS} (L/kg)	0.54	0.3	4.7
IV CL (mL/min/kg)	3.03	0.96	21.57
IV $T_{1/2}$ (h)	2.64	4.47	3.45
Oral $T_{1/2}$ (h)	2.02	4.79	4.43
Oral Bioavailability (F%)	91.98	69.01	86.27

	DSB2455	DSB3218	AZD5305	AZD9574	Olaparib	PARP1 IC_{50} (nM)
PARP1	2	2	9	5	17	
PARP3	743	>5,000	141	>2,000	4	1-9
PARP4	>5,000	>5,000	821	>2,000	13	
PARP5a	3,161	635	218	>2,000	178	10-99
PARP5b	2,482	506	91	>2,000	45	
PARP6	>5,000	>5,000	1,155	>2,000	1,046	100-999
PARP7	>5,000	465	99	>2,000	23	
PARP8	>5,000	>5,000	1,155	>2,000	111	>1000
PARP10	>5,000	>5,000	433	>2,000	325	
PARP11	>5,000	467	9	>2,000	35	
PARP12	>5,000	>5,000	4	>2,000	45	

PARP1 Fold Selectivity

Table 3. DSB2455 & DSB3218 exhibit excellent selectivity over other PARP proteins in NanoBRET[2] assays. [2]Performed at Promega Corp.

Fig. 2. DSB2455 and ATR inhibitors Camonsertib & Ceralasertib combine to potently arrest growth[3] of ATM-deficient NCI-H23 lung cancer cells. [3]7-day CTG viability assay

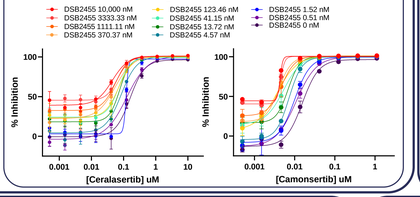

Surface Plasmon Resonance

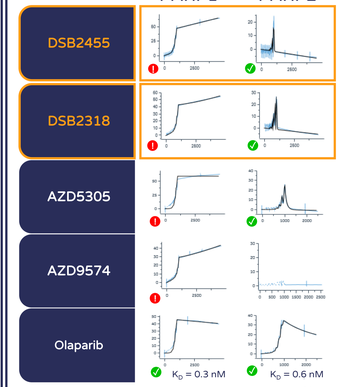

Fig. 3. DSB2455 demonstrates high affinity and prolonged residence time in surface plasmon resonance binding assays.

High affinity with very slow off-rate (no dissociation observed within 1 hr), unable to derive kinetic binding parameters.

In vivo Efficacy

Fig. 4a

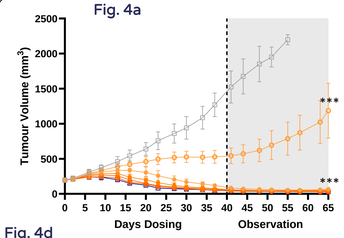

Fig. 4b

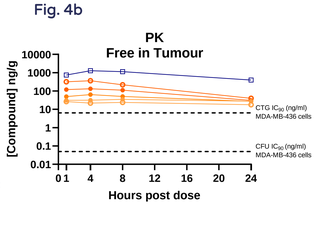

Fig. 4c

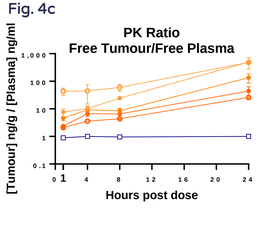

Fig. 4d

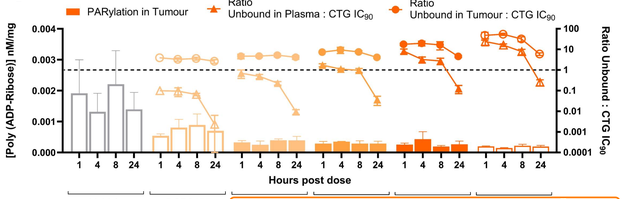

Fig. 4. DSB2455 drives rapid and durable tumour regression in a dose-dependent manner in an MDA-MB-436 breast cancer xenograft model (**Fig. 4a**), demonstrating prolonged tumour residence time at all doses tested (**Fig. 4b**), with superior tumour to plasma ratio (**Fig. 4c**). PARylation was strongly inhibited in tumour (bars) with excellent target coverage (IC_{90}) unbound in both plasma (ng/ml; triangles) and tumour (ng/g; circles) (**Fig. 4d**).

DSB3218 demonstrated similar efficacy profile (data not shown).

Fig. 5a

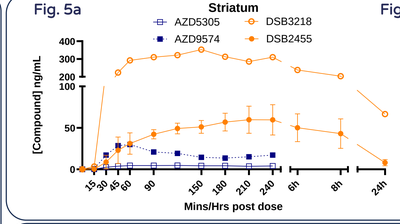

Fig. 5b

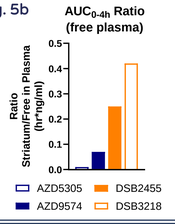

Fig. 5. DSB2455 & DSB3218 demonstrate superior brain penetrance vs AZD9574 following single oral dose of 10 mg/kg in rats (**Fig. 5a**). Compound levels measured following microdialysis of interstitial fluid in striatum. **Fig. 5b.** AUC ratio striatum : free in plasma.

Fig. 6a

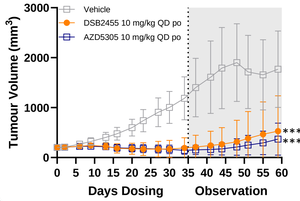

Fig. 6b

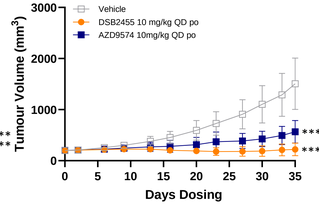

Fig. 6. DSB2455 demonstrates significant anti-tumour efficacy in a Capan-1 pancreatic adenocarcinoma xenograft model (BRCA2$^{-/-}$, KRAS^{G12V}). Efficacy was comparable to AZD5305 (**Fig. 6a**) & superior to AZD9574 (**Fig 6b**).

***p<0.0001 vs vehicle

Fig. 7a

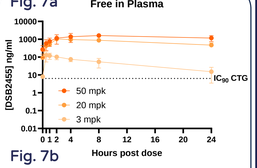

Fig. 7b

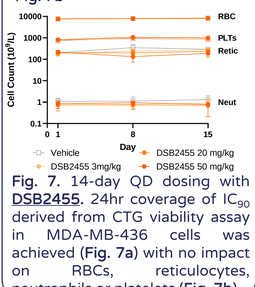

Fig. 7. 14-day QD dosing with DSB2455. 24hr coverage of IC_{90} derived from CTG viability assay in MDA-MB-436 cells was achieved (**Fig. 7a**) with no impact on RBCs, reticulocytes, neutrophils or platelets (**Fig. 7b**).

Summary

We describe the characterization of novel CNS-penetrant, potent and selective PARP1 inhibitors. These molecules demonstrate excellent *in vitro* ADMET, *in vivo* PK and CNS penetrance, coupled with profound anti-tumour efficacy and tumour-targeting properties in genetically-defined mouse models. Our data predict low therapeutic dosing with the potential to demonstrate improved efficacy and tolerability compared to marketed PARP inhibitors, supporting progression of these compounds into clinical studies.

Acknowledgements

Biochemical and biophysical assays were carried out by Proteros Biostructures GmbH; nanoBRET assays were performed by Proteros and Promega Corp; PARP trapping studies were performed by Sai Life Sciences Ltd; *in vitro* biology, ADME, PK and *in vivo* studies were conducted by BioDuro-Sundia and Pharmaron; microdialysis was performed by Pharmidex Pharmaceutical Services Ltd.

#Corresponding author

Alan Wise, PhD. CEO, Duke Street Bio Ltd.
awise@dukesb.com
www.dukestbio.com